Soft Matter

View Online
Dynamic Article Links

Cite this: *Soft Matter*, 2011, **7**, 61

www.softmatter.org

COMMUNICATION

Dendrimer-induced DNA bending†

Chun-Yu Chen,[a] Chun-Jen Su,[b] Shu-Fen Peng,[a] Hsin-Lung Chen*[a] and Hsing-Wen Sung*[a]

Received 11th July 2010, Accepted 21st October 2010
DOI: 10.1039/c0sm00665c

Published on 08 November 2010 on http://pubs.rsc.org | doi:10.1039/C0SM00665C
Downloaded by Synchrotron Radiation Library on 09 February 2011

Depending on the dendrimer charge density (CD), the complexes of DNA with polyamidoamine G4 dendrimer exhibited three distinct nanostructures, characterized by different degrees of DNA bending. With increasing CD, the structure transformed from a square columnar mesophase to hexagonally-packed superhelices and eventually to a beads-on-string structure in which DNA wrapped around the dendrimer by 1.4 turns and penetrated into the dendrimer interior.

Dendrimers are a unique type of hyperbranched macromolecule with perfectly symmetric branching from a central core. The tunable size and surface functionality coupled with the loose internal space allows dendrimers to act as both nanocontainers and surface-active colloids for various biomedical applications. Polyamidoamine (PAMAM) dendrimers, in particular, bear amine groups at the surface and interior, which can be protonated in acidic aqueous media,[1] to generate macrocations capable of forming electrostatic complexes (called "dendriplexes") with DNA for gene delivery.[2] The structures of the dendriplexes at different levels can influence their interaction with cell membranes for endocytosis and the subsequent intracellular release of DNA; however, the supramolecular structures of dendriplexes have been explored predominantly by theoretical simulations.[3–6] There exists an increasingly large gap between the theoretical prediction and the experimental resolution of dendriplex structure, and even the influences of the basic system parameters, such as dendrimer generation number, charge density and the charge ratio remain largely unexplored by experimentalists.

DNA–dendrimer complexation is closely related to the problem of the interactions between a semiflexible polyelectrolyte and an oppositely charged sphere, a subject that is also of interest for understanding the compaction of genomic DNA into chromatin.[7] Theoretical studies have predicted that the electrostatic attraction should lead to, more or less, tight wrapping of DNA-like semiflexible polyelectrolytes around the hard charged spheres, yielding the so-called "beads-on-string" structure found in chromatin.[8,9] Nevertheless, recent experimental results denied the universality of such a structure for dendriplexes, as small angle X-ray scattering (SAXS) revealed the formation of columnar mesophases in which the tetragonally- or hexagonally-packed DNA bridged by dendrimers showed a relatively extended conformation.[10–12] This finding suggests that the energy cost for DNA to wrap around the macrocations also plays a crucial role in determining the complex structure.[9] Columnar mesophase and beads-on-string structures may represent the two ends where bending energy and electrostatic attraction dominates, respectively.

In this study, we unravel how the dendrimer charge density can systematically modulate the bending of DNA in dendriplexes formed in pure water. Using synchrotron SAXS and a scattering function calculation of model structures, we will show that the complexes of DNA with the fourth generation (G4) PAMAM dendrimer exhibited three distinct nanostructures characterized by different degrees of DNA bending. Moreover, we will verify an important theoretical prediction that DNA is able to penetrate into the interior of dendrimer[3–6] while wrapping around the dendrimers with high charge densities.

The charge density of the G4 PAMAM dendrimer was characterized by its degree of protonation (dp, the average number fraction of protonated amine groups) determined from the pH of the protonated dendrimer solution; dp = 0.5 which signified complete surface protonation. The nominal N/P ratio of the dendriplex, prescribed by

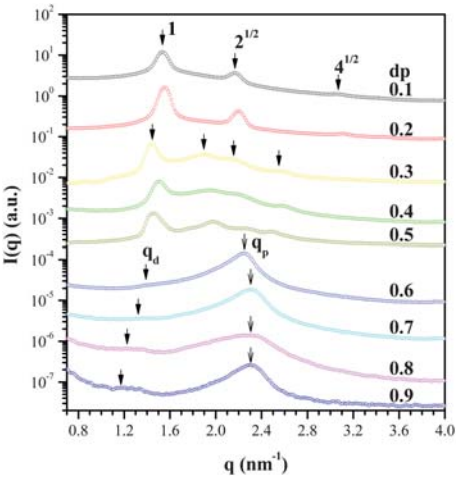

Fig. 1 The SAXS profiles of the dendriplexes with the dendrimer dp values ranging from 0.1 to 0.9. The arrows mark the observable scattering peaks.

[a]*Department of Chemical Engineering, National Tsing Hua University, Hsinchu, 30013, Taiwan. E-mail: hlchen@che.nthu.edu.tw; hwsung@che.nthu.edu.tw*
[b]*National Synchrotron Radiation Research Center, Hsinchu, 300, Taiwan*
† Electronic Supplementary Information (ESI) available: Experimental section, construction of a DNA superhelix for the SAXS profile calculation, calculation of the SAXS profile of a chromatin-like fiber and analysis of the 2-D GISAXS pattern. See DOI: 10.1039/c0sm00665c/

View Online

Published on 08 November 2010 on http://pubs.rsc.org | doi:10.1039/C0SM00665C
Downloaded by Synchrotron Radiation Library on 09 February 2011

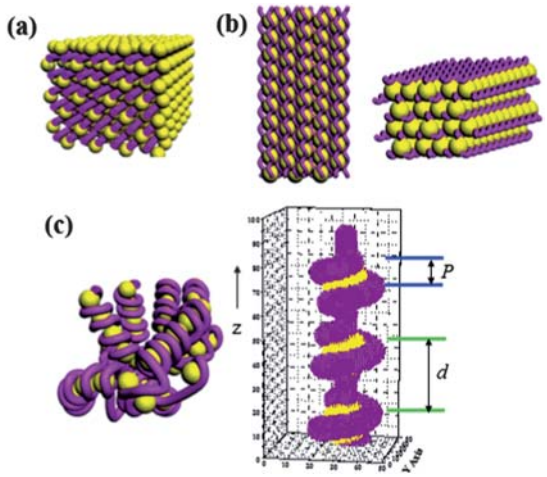

Fig. 2 The schematic illustrations of the three types of nanostructure. (a) The square columnar phase formed at dp < 0.3. (b) The hexagonally-packed DNA superhelices structure formed at dp = 0.3∼0.5. (c) The chromatin-like beads-on-string structure formed at dp ≥ 0.6; *P* and *d* correspond to the pitch length and the axial interparticle distance of the nucleosome-like particles, respectively. The figure on the right shows the actual picture of the chromatin-like segment generated for calculating the SAXS curves.

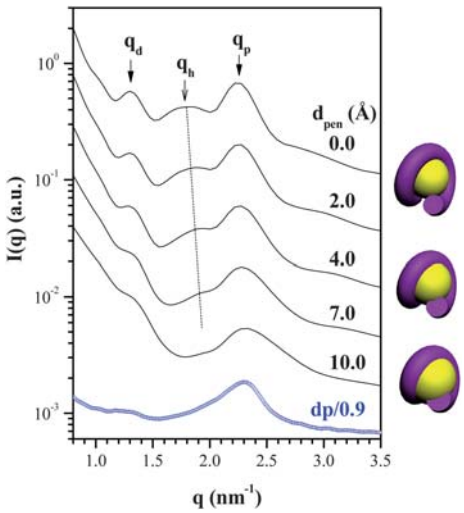

Fig. 3 A comparison of the SAXS profile of the dp/0.9 complex with the calculated scattering curves of the chromatin-like fibers with different penetration depths (d_{pen}) of DNA into the dendrimer. The schemes beside the figure illustrate the nucleosome-like units with different DNA penetration depths.

the feed molar ratio of the amine groups (irrespective of whether they are protonated) to the phosphate groups of DNA, was fixed at 6/1.

Fig. 1 shows the SAXS profiles of the dendriplexes formed at different dp values of the G4 dendrimer in pure water. The scattering profiles of the dp/0.1 and 0.2 complexes exhibited three peaks with the relative positions of $1 : 2^{1/2} : 4^{1/2}$, showing the formation of a square columnar phase with a interhelical distance (d_{DNA}) of 4.11 nm (Fig. 2a).[10–12] The observed d_{DNA} was in close agreement with that calculated *via* $d_{DNA} = (D_{DNA} + D_{den})\cos(45°) = 4.24$ nm with D_{DNA} and D_{den} being the diameter of DNA (= 2 nm) and the dendrimer (= 4 nm),[13] respectively. D_{den} for the neutral dendrimer was adopted in the calculation, as Brownian dynamics simulations revealed that the radius of gyration of dendrimer in the dendriplex with linear polyelectrolyte was close to that for the neutral state.[4]

For dendrimers in which the tertiary amine groups at the interior were protonated (dp ≥ 0.6), the SAXS profiles of the corresponding dendriplexes displayed a strong peak (q_p) at *ca.* 2.3 nm^{-1} and a vaguely identified peak (q_d) at 1.25∼1.45 nm^{-1}. The feature of the scattering pattern was somewhat similar to that of chromatin,[14,15] suggesting that the strong electrostatic attraction induced wrapping of DNA around the dendrimer, yielding the "chromatin-like fiber" composing of the "nucleosome-like" units (Fig. 2c).

The formation of beads-on-string structure was verified by comparing the observed SAXS profiles with the calculated form factor of a chromatin-like fiber. We constructed a chromatin-like rod formed by a DNA chain wrapping around a number of dendrimer macrocations placed along a fiber axis (*i.e.*, z axis) with an axial interparticle distance of *d* (Fig. 2c). Each dendrimer was approximated to be a sphere with the internal monomer density fluctuations,[16] whilst the DNA superhelix was approximated by a uniform helical cylinder with a prescribed pitch length *P* and helix radius R_h (see ESI†).[17] The wrapping was assumed to be tight; therefore, the value of R_h may vary with z. Since *d* was normally larger than D_{den}, a rodlike linker DNA was incorporated between two successive nucleosome-like particles.[18,19]

After assigning the values of *P* and *d*, the system was divided into numerous volume elements and the SAXS profile of the chromatin-like fiber was calculated by the Debye equation[20] (see ESI†). Fig. 3 compares the observed SAXS profile of the dp/0.9 complex with the calculated ones (solid curves) for the chromatin-like fiber composed of six nucleosome-like particles ($P = 2.95$ nm and $d = 5.1$ nm). The uppermost curve corresponded to the case where the DNA superhelix only contacted the surface of the dendrimer while wrapping around it. This calculated profile showed a small lower-q peak and a stronger peak, located at similar positions to those q_d and q_P peaks observed experimentally. The position of q_d was determined by the value of *d* (*i.e.*, $q_d = 2\pi/d$), while that of q_p was determined by the value of *P*. The q_d peak was found to shift progressively to lower q with increasing dp (Fig. 1), while q_p peak moved slightly to higher q (corresponding to a reduction of pitch length) when dp was increased from 0.6 to 0.7, but it stayed invariant with further increase of dp. The length of linker DNA was obtained by $l_{link} = d - D_{den}$; thus, l_{link} increased from 4 Å at dp = 0.6 to 12 Å at dp = 0.9. The observed l_{link} was smaller than that predicted by an analytical model.[19]

The calculated curve contained an additional peak at *ca.* 1.8 nm^{-1} (q_h) not observed clearly in the experimental profile. Previous simulation studies have predicted quite consistently that a polyelectrolyte chain can penetrate into the loose interior of the dendrimer while wrapping around it.[3–6] The effect of such a penetration on the calculated SAXS profile is demonstrated in Fig. 3, where a series of radial penetration depths (d_{pen}) of DNA were further considered for the calculation. It can be seen that q_h shifted to higher q with increasing d_{pen} because the penetration reduced R_h of the DNA superhelix, and it eventually merged with the q_P peak. The fact that the q_h peak was hardly discernible in the experimental SAXS profiles indicated that DNA did penetrate into the dendrimer while wrapping around it and the penetration depth should be larger than 7 Å.

The agreement between the observed SAXS profiles and the calculated scattering curve assuming the beads-on-string structure indicates that DNA was able to wrap around G4 dendrimer with high charge densities (dp ≥ 0.6) as the strong electrostatic attraction

 This journal is © The Royal Society of Chemistry 2011

View Online

Published on 08 November 2010 on http://pubs.rsc.org | doi:10.1039/C0SM00665C
Downloaded by Synchrotron Radiation Library on 09 February 2011

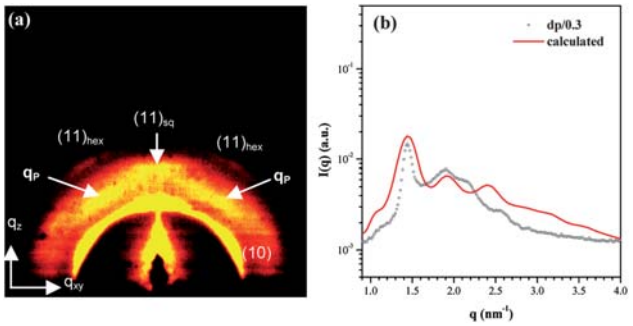

Fig. 4 (a) The GISAXS pattern of a sheared dp/0.3 dendriplex thin film prepared by spreading the dendriplex over a silicon wafer using a blade. The four sets of arcs observed are marked in the pattern. (b) The calculated isotropic SAXS pattern of a hexagonally-packed DNA superhelical structure assuming that the hexagonal lattice consisted of five unit cells with six dendrimer macrocations placing in a given channel.

outweighed the DNA bending energy (or in other words, the chain flexibility of DNA was enhanced by the eletrostatic attraction[3,5,6]). The formation of such a structure in the G4 complex was consistent with the recent theoretical prediction.[19] The number of turns of DNA helically-wrapped around a dendrimer molecule was estimated from the ratio of D_{den} to P, which means that the DNA went one pitch length along the fiber axis to complete one turn in wrapping around the dendrimer. This calculation showed that DNA was wrapped around a dendrimer molecule by *ca.* 1.4 turns.

The SAXS profiles of the dendriplexes with dp values of 0.3∼0.5 exhibited a primary peak at *ca.* 1.44 nm^{-1} and three additional peaks at *ca.* 1.9, 2.1 and 2.5 nm^{-1}. The primary peak was ascribed to spatial correlation of DNA in the complex. The fact that the breadth of this peak was comparable to that associated with the dp/0.1 dendriplex indicated a long-range ordered organization of DNA. In fact, the position ratio of the 2.1 and 2.5 nm^{-1} peaks to the primary peak was about $1 : 2^{1/2}$ and $1 : 3^{1/2}$, respectively, implying that the DNA in the dp/0.3∼0.5 dendriplexes organized in a square and/or a hexagonal lattice. To identify the packing symmetry, we have obtained a two-dimensional SAXS pattern of an anisotropic gel film of the dp/0.3 dendriplex on a silicon wafer using grazing incidence SAXS (GISAXS), as shown in Fig. 4a. Four sets of scattering arcs were identified in the pattern. The first set at *ca.* 1.45 nm^{-1} showed six-fold symmetry, demonstrating that DNA packed predominantly in a hexagonal lattice. The (11) diffraction of the hexagonal lattice was identified as the fourth set of arcs locating at *ca.* 2.5 nm^{-1}. The observed scattering pattern also revealed that DNA in the thin film tended to lie in parallel to the substrate surface.

The 1.9 nm^{-1} peak was not determined by the higher-order diffraction of any two-dimensional lattice. The foregoing analysis of the beads-on-string structure showed that the bending of DNA into a superhelix could give rise to a pitch peak at $q_p = 2\pi/P\cos\theta$, with θ being the pitch angle (see ESI†).[17] Therefore, we postulated that the electrostatic attraction with the dp/0.3∼0.5 dendrimer induced a moderate bending of DNA into superhelices packed in a hexagonal lattice and the 1.9 nm^{-1} peak corresponded to the pitch scattering (Fig. 2b).

The 1.9 nm^{-1} peak corresponded to the second set of arcs (marked by "q_P") locating at the azimuthal angle of 30° in the two-dimensional pattern, signaling that the pitch angle of the DNA superhelices was $\theta \approx 60°$. The pitch length calculated *via* $P = 2\pi/q_p\cos\theta$ was 6.6 nm and R_h [$=P/(2\pi R_h\tan\theta)$][17] of the superhelices was *ca.* 0.6 nm. The small R_h attested that DNA was only slightly twisted for enhancing the charge matching with the dendrimer.

Fig. 4b displays the isotropic SAXS profile associated with the hexagonally-packed DNA superhelices calculated by the Debye equation. For the calculation, DNA superhelices with $P = 6.6$ nm and $\theta = 60°$ were placed in a hexagonal lattice with the interplanar distance of the (10) plane of 4.3 nm. To reach the maximum contact with the dendrimer surface, the phase angle of the DNA superhelix was set to vary in the sequence of +0°, +120°, and +240° along the *a*-axis and *b*-axis of the hexagonal lattice (see ESI†). The dendrimer macrocations were subsequently placed into the groove regions of the channels (each formed by three DNA superhelices). It can be seen that the calculated profile was in qualitative agreement with the observed one. It is noted that the assumed model failed to predict the 2.1 nm^{-1} peak. Considering that the position of this peak was $2^{1/2}$ times that of the primary peak, we suggest that a small amount of the dendriplex might still exhibit the square columnar phase.

In summary, we have shown that the nanostructure of DNA–PAMAM G4 dendrimer complex transformed from a square columnar phase to a hexagonally-packed superhelix and eventually to a beads-on-string structure with increasing dendrimer dp. This structural transition was in accord with the increasing weighting of electrostatic attraction over DNA bending energy with increasing dendrimer charge density. In the beads-on-string configuration, DNA wrapping around each dendrimer by *ca.* 1.4 turns was found to penetrate into the dendrimer and the length of linker DNA increased with increasing dendrimer dp.

References

1 C. J. Su, Y. C. Liu, H. L. Chen, Y. C. Li, H. K. Lin, W. L. Liu and C. S. Hsu, *Langmuir*, 2007, **23**, 975–978.
2 U. Bielinska, C. L. Chen, J. Johnson and J. R. Baker, *Bioconjugate Chem.*, 1999, **10**, 843–850.
3 P. Welch and M. Muthukumar, *Macromolecules*, 2000, **33**, 6159–6167.
4 S. V. Lyulin, A. A. Darinskii and A. V. Lyulin, *Macromolecules*, 2005, **38**, 3990–3998.
5 P. K. Maiti and B. Bagchi, *Nano Lett.*, 2006, **6**, 2478–2485.
6 W. Tian and Y. Ma, *Macromolecules*, 2010, **43**, 1575–1582.
7 K. Zinchenko and D. Yoshikawa, *Phys. Rev. Lett.*, 2005, **95**, 228101.
8 M. Jonsson and P. Linse, *J. Chem. Phys.*, 2001, **115**, 10975–10985.
9 K. K. Kunze and R. R. Netz, *Phys. Rev. Lett.*, 2000, **85**, 4389–4392.
10 Y. C. Liu, H. L. Chen, C. J. Su, H. K. Liu, W. L. Liu and U. Jeng, *Macromolecules*, 2005, **38**, 9434–9440.
11 C. J. Su, H. L. Chen, M. C. Wei, S. F. Peng, H. W. Sung and V. A. Ivanov, *Biomacromolecules*, 2009, **10**, 773–783.
12 H. M. Evans, A. Ahmad, K. Ewert, T. Pfohl, A. Martin-Herranz, R. F. Bruinsma and C. R. Safinya, *Phys. Rev. Lett.*, 2003, **91**, 075501.
13 D. A. Tomalia, A. M. Naylor and W. A. Goddard III, *Angew. Chem., Int. Ed. Engl.*, 1990, **29**, 138–175.
14 J. P. Baldwin, P. G. Boseley and E. M. Bradbury, *Nature*, 1975, **253**, 245–249.
15 J. F. Pardon, D. L. Worcester, J. C. Wooley, R. I. Cotter, D. M. Lilley and R. M. Richards, *Nucleic Acids Res.*, 1977, **4**, 3199–3214.
16 L. Porcar, Y. Liu, R. Verduzco, K. Hong, P. D. Butker, L. J. Magid, G. S. Smith and W. R. Chen, *J. Phys. Chem. B*, 2008, **112**, 14772–14778.
17 I. W. Hamley, *Macromolecules*, 2008, **41**, 8948–8950.
18 S. V. Larin, A. A. Darinskii, A. V. Lyulin and S. V. Lyulin, *J. Phys. Chem. B*, 2010, **114**, 2910–2919.
19 K. Qamhieh, T. Nylander and M.-L. Ainalem, *Biomacromolecules*, 2009, **10**, 1720–1726.
20 P. Debye, *Annalen der Physik*, 1915, **46**, 809–823.